Forsström, Petri R.; Juola, Jussi; Rautiainen, Miina

Relationships between understory spectra and fractional cover in northern European boreal forests

Published in:
Agricultural and Forest Meteorology

DOI:
10.1016/j.agrformet.2021.108604

Published: 15/10/2021

Document Version
Publisher's PDF, also known as Version of record

Agricultural and Forest Meteorology 308-309 (2021) 108604

Contents lists available at ScienceDirect

Agricultural and Forest Meteorology

journal homepage: www.elsevier.com/locate/agrformet

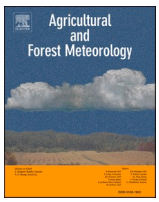

Short communication

Relationships between understory spectra and fractional cover in northern European boreal forests

Petri R. Forsström [a,*], Jussi Juola [a], Miina Rautiainen [a,b]

[a] Department of Built Environment, Aalto University, P.O. Box 14100, 00076 AALTO, Finland
[b] Department of Electronics and Nanoengineering, Aalto University, P.O. Box 15500, 00076 AALTO, Finland

ARTICLE INFO

Keywords:
Forest reflectance
Forest site type
Vegetation index
Hyperspectral

ABSTRACT

Modern satellite and airborne optical images have increasingly higher resolutions and enable the study of all layers of forests, not just the forest canopy. To understand the contribution of different types of understory on the overall spectral reflectance signal, ground reference data are needed from different types of forests. In this paper, we present the analysis of spectral reflectance factors (350-2300 nm) and fractional covers of understory from 36 boreal forest stands. The data were collected during peak growing season in a southern boreal forest area in Finland. The study stands represent four different forest site fertility types. We used a spectrometer to measure understory spectra in nadir and vegetation quadrats to estimate fractional cover. We showed that the understory has specific spectral features related to the site fertility type and fractional cover. Our results suggest that remote sensing can be used to differentiate forest site fertility types and estimate understory green fractional cover in northern European boreal forests. The collected data are openly available in an open data repository.

1. Introduction

Satellite and airborne images may be used for studying the optical and structural properties of all forest layers, not just canopies. Retrieval of understory properties from optical remote sensing data has been shown to be feasible (e.g., Canisius and Chen, 2007; Pisek et al., 2012; Pisek et al., 2016; Kuusk et al., 2018, Markiet & Mõttus, 2020; Pisek et al., 2021). The contribution of understory to the overall forest reflectance can be large and seasonally dynamic (Pisek et al., 2012; Rautiainen and Lukeš, 2015). Although understory is a major component of boreal forest biodiversity, as well as a driver for various forest ecosystem processes (Nilsson and Wardle, 2005), a comprehensive characterization of its spectra in different forest site types is currently missing.

Understory vegetation plays a key role also in practical forest management systems. For example, in Finland, the classification of forests is based on the theory of forest site types (Cajander, 1926), which directly relates understory species composition to forest productivity. According to Cajander's theory, (i) similar growing conditions in forests yield similarities in the compositions of understory vegetation communities; and (ii) the presence of certain understory plant species (i.e., indicator plants) can be used to estimate and predict the productivity metrics of a forest, such as tree height and basal area. Thus, a forest site type is also a proxy for site fertility type (i.e., nutrient and moisture content of soil). Based on this, we hypothesize that understory in different boreal forest site types should have distinct spectral features. If such dependencies exist, they could be applied in future remote sensing applications to map forest site fertility type.

While the species composition of northern European boreal forest understory has been extensively studied (e.g., Majasalmi & Rautiainen, 2020; Tonteri et al., 2016), information on features responsible for variation of spectra within and between different forest site types are missing. Typically, spectral field measurements are expensive and time-consuming to make and thus, are limited to a relatively small number of forest sites (e.g., Rautiainen et al., 2011; Nikopensius et al., 2015). Preceding understory spectral measurements have been mostly made in the visible (VIS) and near-infrared (NIR) spectral regions, 350–1000 nm (e.g., Miller et al., 1997; Rautiainen et al., 2011; Pisek et al., 2021) and thus, data in the shortwave-infrared (SWIR, 1000–2500 nm) region are scarcely available (Peltoniemi et al., 2005; Yang et al., 2014). In addition, spectral data are not solely collected in natural conditions but also in a laboratory (Peltoniemi et al., 2005; Forsström et al., 2019; Kuusinen et al., 2020) and in situ using an artificial light source (Peltoniemi et al., 2005; Yang et al., 2014). Further, so far only

* Corresponding author.
E-mail addresses: petri.forsstrom@aalto.fi (P.R. Forsström), jussi.juola@aalto.fi (J. Juola), miina.a.rautiainen@aalto.fi (M. Rautiainen).

https://doi.org/10.1016/j.agrformet.2021.108604
Received 2 March 2021; Received in revised form 29 July 2021; Accepted 8 August 2021
Available online 20 August 2021

some of the collected understory spectral data are made openly available through data repositories to encourage data reuse.

In this paper, we present the first analysis of the relationships between nadir view spectral properties and fractional covers of four boreal forest site types in the VIS, NIR, and SWIR spectral regions. We measured a spectral library and fractional cover of 36 forest stands in Finland during the peak growing season. Our research questions were, (i) what are the spectral characteristics of different forest site types? (ii) how large is the variation of the understory spectra both within and between different forest site types? (iii) how are the spectral properties and fractional cover of understory related to each other in different site types? The spectral library is available as open data (Forsström et al., 2021).

2. Materials and methods

2. 1. Study area

We conducted field measurements in southern boreal forests near the Hyytiälä Forestry Field Station (61°50'N, 24°17'E) in Finland during summers of 2018 and 2019. We selected 36 forest stands with different characteristics and classified them into four upland (mineral soil) forest site types based on Cajander's theory (1926): 1. *Oxalis-Myrtillus* type (OMT), i.e., moderately-rich upland sites dominated by dense populations of graminoids, ferns, and blueberry shrubs; 2. *Myrtillus* type (MT), i.e., moist upland sites dominated by moderately rich populations of blueberry shrubs and moss; 3. *Vaccinium* type (VT), i.e., dryish upland sites dominated by widely spread lingonberry shrubs and moss; 4. *Calluna* type (CT), i.e., dry upland sites dominated by moss, small size lingonberry shrubs and lichen (Fig. 1). In previous studies (cf. Rautiainen et al., 2011; Majasalmi & Rautiainen, 2020), these site types have been referred to as herb-rich (OMT), mesic (MT), sub-xeric (VT) and xeric (CT) sites. The dominant tree species in the study stands were Norway spruce (*Picea abies* (L.) Karst), silver birch (*Betula pendula* Roth), and Scots pine (*Pinus sylvestris* L.).

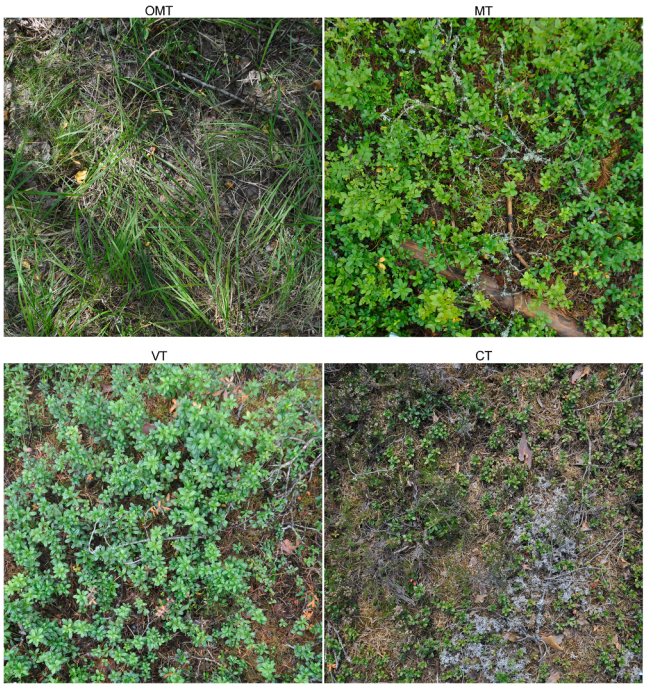

Fig. 1. Photos of ground cover in the four boreal forest site types included in this study, with typical fractional covers of different understory components (see Table 1). The fractional covers estimated from the photos are for Oxalis-Myrtillus type (OMT) 57/43/0, Myrtillus type (MT) 76/24/0, Vaccinium type (VT) 81/19/0, and Calluna type (CT) 60/27/13 [%] for green vegetation, plant litter, and lichen, respectively.

The ground cover in the more fertile OMT and MT sites is characterized by a richness of vascular plant species, strong variation of fractional cover between green vegetation and plant litter within and between sites, and a strongly heterogenous and complex understory canopy structure. In contrast, the ground in the less fertile VT and CT sites is more uniformly covered by moss, dwarf shrubs are smaller in size, and the understory canopy is spatially more homogenous.

2.2. Measurements and processing of spectra

In each study site, we established a 11 m long East-West transect, used in the nadir view understory measurements and to conduct routine forest inventory around the transect (Table 1). Each transect was divided into 15 evenly spaced sampling positions (~80 cm apart). Natural variations in the topography of the ground did not affect the placement of a transect, unless they prevented making measurements. During the measurements, understory was kept intact by standing only on the North-side of a measurement transect. The spectra were collected always under natural diffuse illumination.

We used ASD's FieldSpec4 spectrometer (350–2500 nm) (serial number 18456) with bare fiber sensor optics and a pistol grip in a backpack measurement set-up. The opening angle of the sensor was 25 degrees and the resulting sensor footprint approximately 50 cm in diameter, depending on microtopography. We saved 15 averaged understory spectra of each transect (one from each sampling position). The integration time was optimized for each transect by measuring a signal from a white reference panel (Spectralon®, 99% nominal reflectance). Maximum integration time of 2.18 s was used in order to keep the time between understory spectra and reference spectra measurements relatively short while still achieving acceptable signal quality, based on visual judgement. Reference spectra were measured from the white reference panel always at the first and last sampling positions, as well as in every third position on the transect. During the reference measurement, the white reference panel was held by a co-operator, at approximately 0.5 m above the ground next to the understory spectra sampling position, and a bubble level was used to adjust the white reference panel horizontal. From each of the reference measurement positions, we saved three spectra. Additionally, we also measured dark current spectra before and after the other spectral measurements in order to remove the effect of the inherent off-set signal by the spectrometer. Measuring one transect took ~23 minutes to complete.

The sensor readings from the spectrometer, i.e., the measurement data in digital numbers (DN), were processed to hemispherical-conical reflectance factors (HCRF) (Schaepman-Strub et al., 2006) by assuming corresponding illumination and measurement geometries. We will refer to HCRF simply as reflectance factor (RF). The processing steps for the spectral data from each transect were the following: First, the sensor readings of the wavelength dependent dark currents were averaged per wavelength to produce a spectral reading which was subtracted from all white reference and understory spectral readings; Second, each understory spectral reading was divided by the white reference reading from the closest position, resulting in spectral RFs; Third, the RFs were filtered with Savitzky-Golay algorithm (51 nm window); Fourth, the filtered RFs from each measurement position were averaged to a mean spectrum of the transect. For each transect, the temporal stability of the sensor was verified by comparing the dark current readings made before and after the understory spectral measurements. Furthermore, data in the spectral regions of high atmospheric noise, i.e., 1321–1509 nm, 1771–2099 nm, 2301–2500 nm were excluded from analyses. In addition, data in the spectral range 2100–2300 nm from selected measurement positions in one OMT, four MT, one VT, and one CT transects were as well excluded due to high noise by low irradiance at the time of measurement. Standard deviation and coefficient of variation (CV) were calculated for each site type based on the mean RFs of each transect.

The mean RFs and their variation were analyzed in full spectral

Table 1
Forest site characteristics for tree and understory layers. Forest site types are Oxalis-Myrtillus type (OMT), Myrtillus type (MT), Vaccinium type (VT), and Calluna type (CT). Measurement data are given as means with data ranges [in brackets] or standard deviations (in parentheses).

		Tree layer characteristics						Understory characteristics		
Forest site type	Number of sites	Pine [%]	Spruce [%]	Birch [%]	Other tree species [%]	Basal area [m^2/ha]	Median tree height [m]	Green vegetation cover [%]	Litter cover [%]	Lichen cover [%]
OMT (most fertile)	11	1 [0-8]	50 [0-99]	48 [0-100]	2 [0-14]	27 [11-50]	23 [17-34]	59 (20)	42 (20)	0 (0)
MT	11	27 [0-99]	62 [0-97]	9 [1-23]	2 [0-18]	31 [22-36]	22 [15-29]	73 (15)	27 (15)	0 (0)
VT	9	95 [63-100]	4 [0-33]	0 [0-4]	1 [0-5]	24 [5-48]	19 [7-25]	81 (10)	19 (10)	0 (0)
CT (least fertile)	5	100	0	0	0	21 [19-23]	19 [12-25]	60 (15)	26 (5)	14 (11)

resolution. We assessed the effect of fractional cover on the variation of spectra. In addition, we examined the spectral shift of the red edge position (REP) for each site type using the linear four-point interpolation method (Guyot et al., 1992). Further, we calculated all narrowband normalized difference indices (NDI) for each forest site type. As an example of a data application, we then evaluated the performance of corresponding linear regression models to explain the variation in green fractional cover, and compared the performance of the NDI-of-best-fit for pooled data and a commonly used broadband NDI, i.e., normalized difference vegetation index (NDVI) (Rouse et al., 1974). NDI was always calculated from RFs in single wavelengths (λ) as ($RF_{\lambda 2}$ - $RF_{\lambda 1}$) / ($RF_{\lambda 2}$ + $RF_{\lambda 1}$). NDVI was calculated using the mean RFs (±5 nm) in the red (665 nm) and NIR (835 nm) spectral ranges.

2.3. Measurements and processing of fractional cover

To estimate the fractional cover for a transect, a wooden frame of size 1 m x 1 m was placed on the ground and a digital system camera (Nikon D5000) was used to photograph it from nadir at four sampling positions along the transect. The quadrat photos were rectified and cropped in

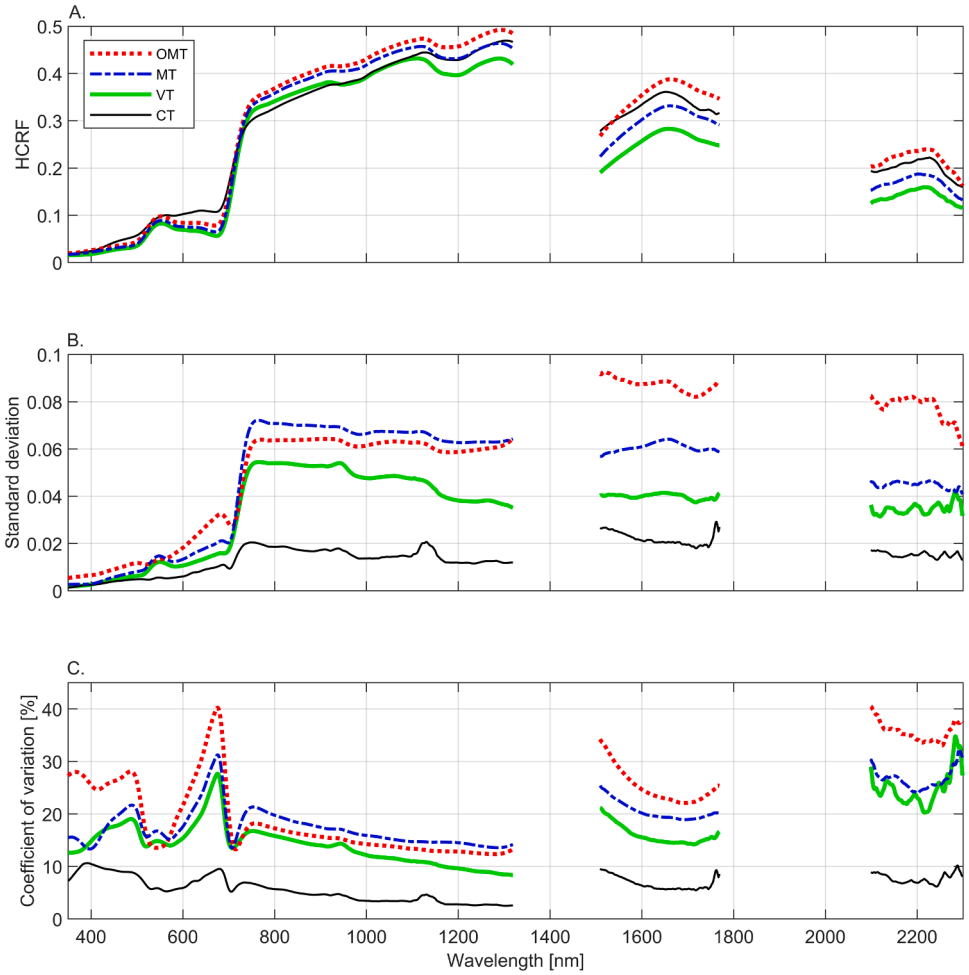

Fig. 2. Understory reflectance spectra (350–2300 nm) of four forest site types: A. mean hemispherical-conical reflectance factors (HCRF) for each forest site type, B. corresponding standard deviations, C. corresponding coefficients of variation. The forest site types are Oxalis-Myrtillus type (OMT), Myrtillus type (MT), Vaccinium type (VT), Calluna type (CT). Spectral data are excluded in wavelengths with high atmospheric noise.

post-processing, and overlaid with a 10 cm x 10 cm grid so that each subsection of the grid represented one percent of the total image area. The sub-sections were then classified by a visual method (by the same person) into one of three fractional cover classes: green vegetation, plant litter, or lichen. Finally, the fractional cover of a transect was calculated as the mean of fractional covers of the quadrats, and fractional cover of a site type as the mean fractional cover of the transects (Table 1).

3. Results and discussion

In OMT sites, green vegetation covered about half (59%) of the ground, while the other half was litter (Table 1). In MT and VT sites, the fraction of green vegetation was higher (73% and 81%, respectively). CT was the only site type with lichen cover (14%), complemented by green vegetation (60%) and litter (26%). The most fertile site type OMT had the largest variation in the fractional cover between the transects and the less fertile site type VT the smallest variation.

There were similarities as well as distinguishing differences between the nadir view mean spectra of the forest site types (Fig. 2a). In both VIS (350–700 nm and red edge 700–800 nm) and NIR (800–1300 nm), the spectra of OMT, MT, and VT sites resembled that of healthy green leaves (i.e., low RF in the blue and red wavelengths, and high RF in NIR), while all site types, including CT showed decreasing trend of RFs in SWIR (1300–2300 nm). CT sites exhibited less pronounced absorption spectra in VIS compared to other site types, a spectral characteristic typical to lichen (Kuusinen et al., 2020). The largest variation in spectra within a forest site type was for OMT sites in VIS and SWIR, and for MT sites in NIR (Fig. 2b–c). CT sites had always the smallest variation in spectra. The difference in the level of variations between the forest site types was related to the variation in the fractional cover and may have been affected by the variation in the dominant plant type (i.e., dwarf shrubs, ferns, graminoids, and mosses). Next, we will discuss in more detail the spectral behavior of the site types in the VIS, red edge, NIR, and SWIR spectral regions.

Larger green fractional cover resulted in lower RF in VIS for all site types except for CT (Fig. 2a). This can be explained by the optical properties of understory green leaves that effectively lower the RF in more closed understory canopies: e.g., a dwarf shrub leaf may absorb nearly all (~90%) of the incident VIS radiation (Forsström, 2018). In contrast, the green fractional covers in CT sites consisted mainly of moss with characteristic high reflectance in VIS (Bubier et al., 1997).

Throughout the red edge spectral region, RFs increased rapidly for all site types (Fig. 2a) and the REPs were between 714 and 720 nm for all stands (Fig. 3). Subtle differences were noted when comparing REPs between the site types: CT 715–717 nm, VT 716–718 nm, MT 715–718 nm, and OMT 714–720 nm. Similar dynamics of REP for boreal forests have been reported also previously (Rautiainen et al., 2011; Nikopensius et al., 2015).

In NIR, the OMT site type was brighter than the other site types (Fig. 2a). Since OMT sites had the smallest fractional cover of green vegetation, and correspondingly, the largest fractional cover of litter (typically characterized by relatively low NIR reflectance (Forsström et al., 2019), the properties of the understory canopy structure may have influenced the spectra more than in other site types. Based on visual observations, the understory canopies in OMT and MT sites were clumped (i.e., dense) and multi-layered. Furthermore, RF in CT sites increased strongly from the shorter to longer wavelength-edge in the NIR region which may have been due to a relatively larger contributions of moss, litter, and dry soil under the low-growing understory canopy.

In SWIR, the site types that had large green fractional cover were darker (Fig. 2a). In general, the low RFs in SWIR were likely due to the strong spectral absorption feature of water which increases as a function of wavelength (e.g., Ustin et al., 2012). Thus, the variation of spectra in SWIR between the site types was probably affected more by the variation in the green fractional cover than structural properties of the understory canopy. Furthermore, we speculate that the water-retaining

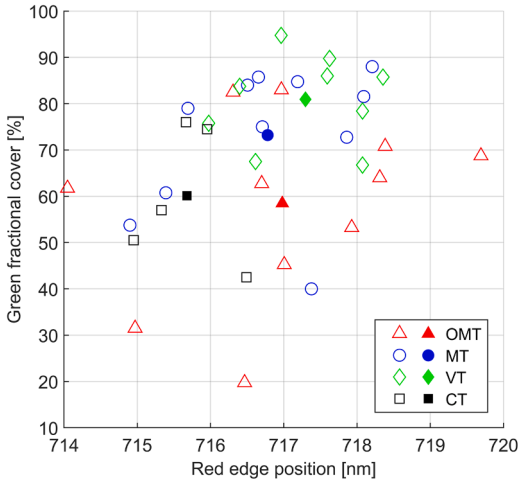

Fig. 3. Red edge positions in relation to green fractional cover of understory of study stands. The four different forest site types are Oxalis-Myrtillus type (OMT), Myrtillus type (MT), Vaccinium type (VT), Calluna type (CT). Empty symbols are for individual sites and filled symbols show the mean values of each site type.

characteristics of soils in different site types influenced the RFs in SWIR more than elsewhere in the spectrum (OMT and MT sites are characterized by moist soil, VT sites by dryish soil, and CT sites by dry soil).

The spectral reflectance characteristics of the site types in the VIS to NIR wavelengths were similar to those reported previously from the same forest area during peak growing season (Fig. 3c in Rautiainen et al., 2011). While a direct comparison of the results between studies with different measurement protocols has its difficulties (e.g., Rautiainen et al. (2011) studied the seasonality of understory spectra only in a single study stand per forest site fertility type), the abundance of vascular green vegetation may be seen to increase red-light absorption and NIR reflectance in understory spectra, while a larger ground coverage of moss and lichen reduces those effects.

Next, we further examined the relationships between the nadir view spectral properties and fractional covers. We used two linear regression models based on NDI and NDVI to predict green fractional cover for pooled data from all stands (Figs. 4a, 5) and for each forest site type individually (Fig. 4b–e). The NDIs based on RFs in the long-wave ultraviolet (380–430 nm) wavelengths and NIR (715–1320 nm) had the strongest relationship with green fractional cover in the pooled data ($R^2 > 0.7$) (Fig 4a), with the single wavelength-specific NDI-of-best-fit ($\lambda_1 = 957$ nm, $\lambda_2 = 406$ nm; $R^2 = 0.74$, RMSE = 8.86%) (Fig. 5) being strongly related to green fractional cover in OMT ($R^2 \approx 0.82$) (Fig. 4b), VT ($R^2 \approx 0.75$) (Fig. 4d), and CT ($R^2 \approx 0.94$) (Fig. 4e) sites, while less so for MT sites ($R^2 \approx 0.35$) (Fig. 4c). We speculate (based on visual observations) that the result for MT sites may have been influenced by a high diversity of plant types: there were tall grasses and blueberry shrubs in areas with more light and relatively uniform moss cover elsewhere.

Models of NDI-of-best-fit were also determined for each forest site type individually. Overall, the individual relationships between the green fractional cover and NDI-of-best-fit were strong for all site types ($R^2 > 0.88$) (Fig. 4b–e). OMT sites (Fig. 4b) had a wider range of well performing spectral combinations compared to the second most fertile site type MT for which the applicable combinations were scarcer and located solely in SWIR (Fig. 4c). For the less fertile VT site type (Fig. 4d), the most useful combinations were found in VIS and SWIR, and for CT sites (Fig. 4e), in VIS and NIR. It should be noted that although the model of NDI-of-best-fit for CT sites seemed to perform very well, the number of sites included in the fitting was the smallest (4). In general, CT sites are rare in southern boreal zone in Finland (accounting for less than 2% of forest land (Hotanen et al., 2008).

The relationship between green fractional cover and NDVI, on the

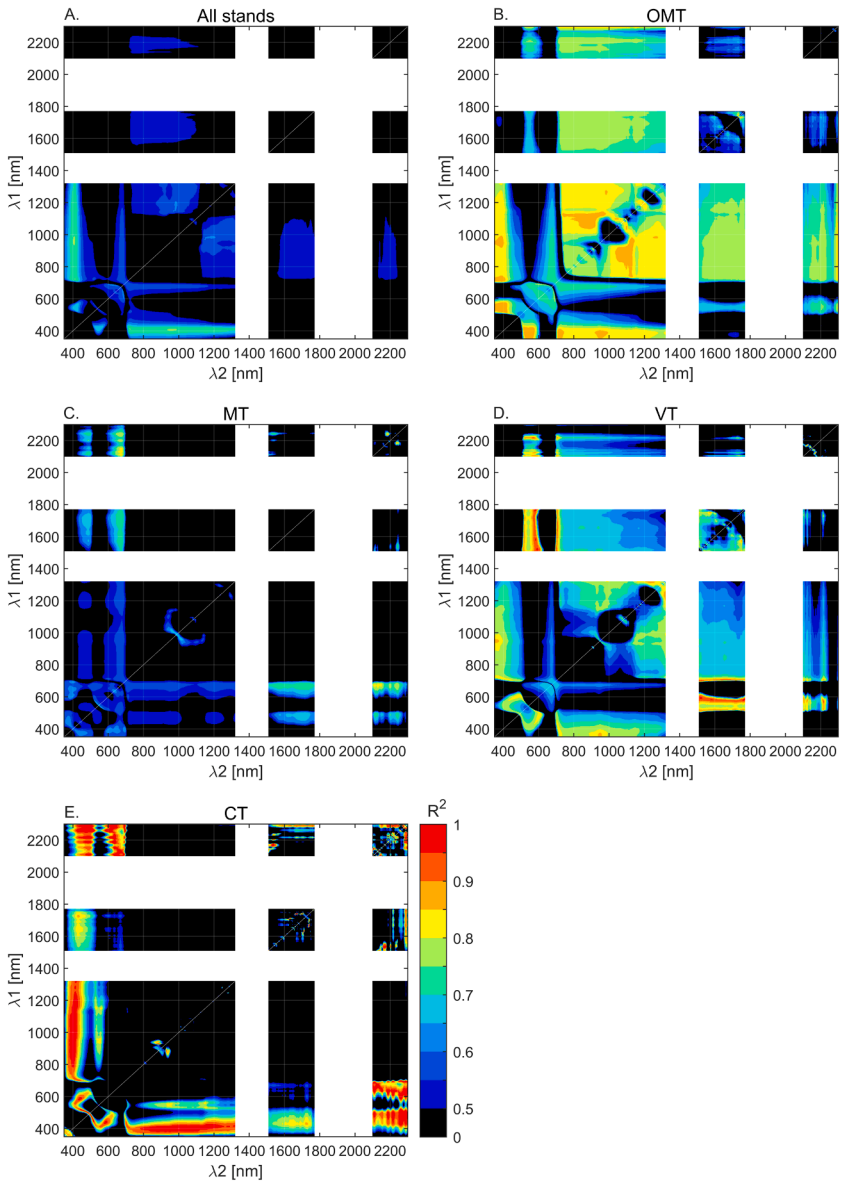

Fig. 4. Coefficients of determination (R^2) for all possible spectral combinations ($\lambda 1$, $\lambda 2$) (350–2300 nm) in narrowband normalized difference index (NDI) and the observed green fractional cover: A. for all stands, B–E. for four forest site types individually. The forest site types are Oxalis-Myrtillus type (OMT), Myrtillus type (MT), Vaccinium type (VT), Calluna type (CT). NDI is calculated from the mean hemispherical-conical reflectance factors (HCRF) of each forest site type as ($HCRF_{\lambda 2}$ - $HCRF_{\lambda 1}$) / ($HCRF_{\lambda 2}$ + $HCRF_{\lambda 1}$). Spectral data are excluded in wavelengths with high atmospheric noise.

other hand, was clearly weaker for pooled data from all stands ($R^2 \approx 0.55$, RMSE =11.69%) (Figs. 4a, 5), and was particularly poor in CT sites ($R^2 = 0.18$) (Fig. 4e). The poor fit of NDVI in CT sites could be related to the contrast between the similar spectral characteristics of moss (Bubier et al., 1997; Peltoniemi et al., 2005), litter (Forsström et al., 2019) and lichen (Kuusinen et al., 2020), and the relatively large variation between the fractional covers (Table 1).

Our results show that the optimal wavelengths for estimating understory green fractional cover are different for each forest site type and are in relatively narrow spectral ranges in VIS, NIR, and SWIR regions (Fig. 4b-e). This suggests that in remote monitoring of understory greenness in different types of forests, whether made from above or under the tree canopy, the spectral data should be collected in sufficiently high spatial resolution and with wide enough spectral coverage, extending into the SWIR region. While understory spectral reflectance may be retrieved for large areas even from satellite data with coarse spectral and spatial resolutions (Pisek et al., 2012, 2015, 2016, 2021), fortunately, there is also an increasing interest in developing small-size spectral cameras for UAV-platforms (e.g., Ziph-Schatzberg et al., 2018, Jenal et al., 2019, Li et al., 2021). The flexibility of UAV measurements methods for collecting data in centimeter scale spatial resolution (Näsi et al., 2016, Fawcett et al., 2020) are needed for detecting, e.g., subtle phenological changes in understory vegetation (Forsström et al., 2019). While to date, data from spaceborne hyperspectral instruments have been scarce (PROBA/CHRIS, EO-1/Hyperion), studies have already shown the potential of high resolution satellite data in separating the contributions of forest tree canopy and understory layers from the overall forest reflectance (Rautiainen et al., 2008, Rautiainen & Lukeš, 2015). Now that new spaceborne hyperspectral instruments are being deployed (e.g., PRISMA (Loizzo et al., 2018), EnMAP (Guanter et al., 2015)), development of new applications for mapping characteristics of also forest understory become again topical.

4. Conclusions

We showed that northern European boreal forest understory spectra, collected in nadir view direction and during peak growing season, depend on site fertility. Based on our results, different forest site types have specific spectral characteristics that are linked to the fractional covers of their understory. Our results suggest, for the first time, that measuring understory spectra beyond the conventional VIS-NIR spectral region may enable retrieving information on forest site fertility types.

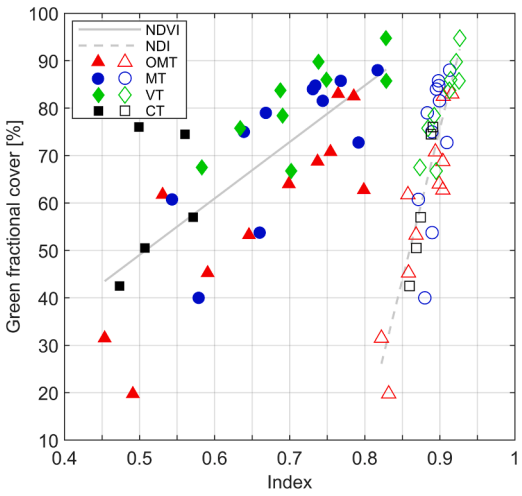

Fig. 5. Two linear regression models between the observed green fractional cover and spectral vegetation index from all stands. The models are based on NDI-of-best-fit (957 nm, 406 nm) (gray dashed line) and NDVI (665 ± 5 nm, 835 ± 5 nm) (gray line), calculated from the mean hemispherical-conical reflectance factors (HCRF) of each stand as ($HCRF_{\lambda 2}$ - $HCRF_{\lambda 1}$) / ($HCRF_{\lambda 2}$ + $HCRF_{\lambda 1}$), where λ# are the corresponding wavelengths of each index. The four different forest site types are Oxalis-Myrtillus type (OMT), Myrtillus type (MT), Vaccinium type (VT), Calluna type (CT). Empty symbols are for NDI-based model and filled symbols for NDVI-based model. The NDI-based model for green fractional cover is y = 635.78x - 496.60 [%] (R^2 = 0.74, RMSE = 8.86%) and NDVI-based model y = 119.05x - 10.48 [%] (R^2 = 0.55, RMSE = 11.69%). Empty symbols are for NDI-based model and filled symbols for NDVI-based model.

Mapping forest site types and monitoring changes in understory properties from remote sensing observations could support sustainable forest management actions related to e.g., biodiversity conservation. Further research should be dedicated to incorporating spectral libraries of understory in the analyses of high spatial resolution remote sensing data from forest areas.

Declaration of Competing Interest

The authors declare that they have no known competing financial interests or personal relationships that could have appeared to influence the work reported in this paper.

Acknowledgments

We thank Aarne Hovi, Ville Ranta, and Daniel Schraik for collaboration. This work was supported by the Academy of Finland [BOREALITY, grant number 286390; and DIMEBO, grant number 3323004]; and by the European Research Council (ERC) under the European Union's Horizon 2020 research and innovation programme [grant agreement No 771049]. The article reflects only the authors' view and the Agency is not responsible for any use that may be made of the information it contains.

References

Bubier, J.L., Rock, B.N., Crill, P.M., 1997. Spectral reflectance measurements of boreal wetland and forest mosses. J. Geophys. Res. 102 (D24), 29483–29494. https://doi.org/10.1029/97JD02316.

Cajander, A.K., 1926. The theory of forest types. Acta Forestalia Fennica 29 (3). https://doi.org/10.14214/aff.7193 article id 7193.

Canisius, F., Chen, J.M., 2007. Retrieving forest background reflectance in a boreal region from Multi-angle Imaging SpectroRadiometer (MISR) data. Remote Sens. Environ. 107 (1–2), 312–321. https://doi.org/10.1016/j.rse.2006.07.023.

Fawcett, D., Bennie, J., Anderson, K., 2020. Monitoring spring phenology of individual tree crowns using drone-acquired NDVI data. Remote Sens. Ecol. Conserv. https://doi.org/10.1002/rse2.184.

Forsström, P., 2018. Spectral Bidirectional Reflectance Factor Measurements Of Two Dwarf Shrub Species. Master's thesis. Aalto University. http://urn.fi/URN:NBN:fi:aalto-201802231639.

Forsström, P., Peltoniemi, J., Rautiainen, M., 2019. Seasonal dynamics of lingonberry and blueberry spectra. Silva Fennica 53 (2). https://doi.org/10.14214/sf.10150 article id 10150.

Forsström, P.R., Juola, J., Hovi, A., Rautiainen, M., 2021. Dataset of understory reflectance spectra and fractional cover in a boreal forest area in Finland. Mendeley Data V1. https://doi.org/10.17632/2g9nkcdj53.1.

Guanter, L., Kaufmann, H., Segl, K., Foerster, S., Rogass, C., Chabrillat, S., Kuester, T., Hollstein, A., Rossner, G., Chlebek, C., Straif, C., Fischer, S., Schrader, S., Storch, T., Heiden, U., Mueller, A., Bachmann, M., Mühle, H., Müller, R., Habermeyer, M., Ohndorf, A., Hill, J., Buddenbaum, H., Hostert, P., Van der Linden, S., Leitão, P.J., Rabe, A., Doerffer, R., Krasemann, H., Xi, H., Mauser, W., Hank, T., Locherer, M., Rast, M., Staenz, K., Sang, B., 2015. The EnMAP Spaceborne Imaging Spectroscopy Mission for Earth Observation. Remote Sens. 7 (7), 8830–8857. https://doi.org/10.3390/rs70708830.

Guyot, G., Baret, F., Jacquemoud, S., 1992. Imaging spectroscopy for vegetation studies. In: Toselli, F., Bodechtel, J. (Eds.), Imaging Spectroscopy: Fundamentals and Prospective Applications. Kluwer Academic Publishers, Dordrecht, The Netherlands, pp. 145–165.

Hotanen, J.-P., Nousiainen, H., Mäkipää, R., Reinikainen, A., Tonteri, T., 2008. Metsätyypit – opas kasvupaikkojen luokitteluun. Metsäntutkimuslaitos, Metsäkustannus Oy.

Jenal, A., Bareth, G., Bolten, A., Kneer, C., Weber, I., Bongartz, J., 2019. Development of a VNIR/SWIR multispectral imaging system for vegetation monitoring with unmanned aerial vehicles. Sensors 19, 5507. https://doi.org/10.3390/s19245507.

Kuusinen, N., Juola, J., Karki, B., Stenroos, S., Rautiainen, M., 2020. A spectral analysis of common boreal ground lichen species. Remote Sens. Environ. 247, 111955 https://doi.org/10.1016/j.rse.2020.111955.

Kuusk, A., Pisek, J., Lang, M., Märdla, S., 2018. Estimation of gap fraction and foliage clumping in forest canopies. Remote Sens. 10 (7), 1153. https://doi.org/10.3390/rs10071153.

Li, L., Mu, X., Qi, J., Pisek, J., Roosjen, P., Yan, G., Huang, H., Liu, S., Baret, F., 2021. Characterizing reflectance anisotropy of background soil in open-canopy plantations using UAV-based multiangular images. ISPRS J. Photogramm. Remote Sens. 177, 263–278. https://doi.org/10.1016/j.isprsjprs.2021.05.007.

Loizzo, R., Guarini, R., Longo, F., Scopa, T., Formaro, R., Facchinetti, C., Varacalli, G., 2018. Prisma: The Italian hyperspectral mission. *IGARSS 2018 – 2018 IEEE International Geoscience and Remote Sensing Symposium. IEEE.* https://doi.org/10.1109/IGARSS.2018.8518512.

Majasalmi, T., Rautiainen, M., 2020. The impact of tree canopy structure on understory variation in a boreal forest. Forest Ecol. Manag. 466, 118100 https://doi.org/10.1016/j.foreco.2020.118100, 15 June 2020.

Markiet., V., Mõttus, M., 2020. Estimation of boreal forest floor reflectance from airborne hyperspectral data of coniferous forests. Remote Sens. Environ. 249, 112018 https://doi.org/10.1016/j.rse.2020.112018.

Miller, J.R, White, H.P., Chen, J.M., Peddle, D.R., McDermid, G., Fournier, R.A., Shepherd, P., Rubinstein, I., Freemantle, J., Soffer, R., LeDrew, E., 1997. Seasonal change in understory reflectance of boreal forests and influence on canopy vegetation indices. J. Geophys. Res. 102 (D24), 29475–29482. https://doi.org/10.1029/97JD02558.

Nikopensius, M., Pisek, J., Raabe, K., 2015. Spectral reflectance patterns and seasonal dynamics of common understory types in three mature hemi-boreal forests. Internal J. Appl. Earth Observ. Geoinf. 43, 84–91. https://doi.org/10.1016/j.jag.2014.11.012.

Nilsson, M.-C., Wardle, D.A., 2005. Understory vegetation as a forest ecosystem driver: evidence from the northern Swedish boreal forest. Front. Ecol. Environ. 3 (8), 421–428. https://doi.org/10.1890/1540-9295(2005)003[0421:UVAAFE]2.0.CO;2.

Näsi, R., Honkavaara, E., Tuominen, S., Saari, H., Pölönen, I., Hakala, T., Viljanen, N., Soukkamäki, J., Näkki, I., Ojanen, H., Reinikainen, J., 2016. UAS based tree species identification using the novel FPI based hyperspectral cameras in visible, NIR and SWIR spectral ranges. In: International archives of the photogrammetry, remote sensing and spatial information sciences, Proceedings of the XXIII ISPRS Congress, Volume XLI-B1. https://doi.org/10.5194/isprsarchives-XLI-B1-1143-2016.

Peltoniemi, J.I., Kaasalainen, S., Näränen, J., Rautiainen, M., Stenberg, P., Smolander, H., Smolander, S., Voipio, P., 2005. BRDF measurement of understory vegetation in pine forests: dwarf shrubs, lichen, and moss. Remote Sens. Environ. 94 (3), 343–354. doi:10.1016/j.rse.2004.10.009.

Pisek, J., Rautiainen, M., Heiskanen, J., Mõttus, M., 2012. Retrieval of seasonal dynamics of forest understory reflectance in a Northern European boreal forest from MODIS BRDF data. Remote Sens. Environ. 117, 464–468. https://doi.org/10.1016/j.rse.2011.09.012.

Pisek, J., Rautiainen, M., Nikopensius, M., Raabe, K., 2015. Estimation of seasonal dynamics of understory NDVI in northern forests using MODIS BRDF data: semi-empirical versus physically-based approach. Remote Sens. Environ. 163, 42–47. https://doi.org/10.1016/j.rse.2015.03.003.

Pisek, J., Chen, J.M., Kobayashi, H., Rautiainen, M., Schaepman, M.E., Karnieli, A., Sprinstin, M., Ryu, Y., Nikopensius, M., Raabe, K., 2016. Retrieval of seasonal dynamics of forest understory reflectance from semiarid to boreal forests using MODIS BRDF data. J. Geophys. Res. 121, 855–863. https://doi.org/10.1002/2016JG003322.

Pisek, J., Erb, A., Korhonen, L., Biermann, T., Carrara, A., Cremonese, E., Cuntz, M., Fares, S., Gerosa, G., Grünwald, T., Hase, N., Heliasz, M., Ibrom, A., Knohl, A., Kobler, J., Kruijt, B., Lange, H., Leppänen, L., Limousin, J.-M., Serrano, F.R.L., Loustau, D., Lukeš, P., Lundin, L., Marzuoli, R., Mölder, M., Montagnani, L.,

Neirynck, J., Peichl, M., Rebmann, C., Rubio, E., Santos-Reis, M., Schaaf, C., Schmidt, M., Simioni, G., Soudani, K., Vincke, C., 2021. Retrieval and validation of forest background reflectivity from daily Moderate Resolution Imaging Spectroradiometer (MODIS) bidirectional reflectance distribution function (BRDF) data across European forests. Biogeosciences 18, 621–635. https://doi.org/10.5194/bg-18-621-2021.

Rautiainen, M., Lang, M., Mõttus, M., Kuusk, A., Nilson, T., Kuusk, J., Lükk, T., 2008. Multi-angular reflectance properties of a hemiboreal forest: an analysis using CHRIS PROBA data. Remote Sens. Environ. 112 (5), 2627–2642. https://doi.org/10.1016/j.rse.2007.12.005.

Rautiainen, M., Mõttus, M., Heiskanen, J., Akujärvi, A., Majasalmi, T., Stenberg, P., 2011. Seasonal reflectance dynamics of common understory types in a northern European boreal forest. Remote Sens. Environ. 115 (12), 3020–3028. https://doi.org/10.1016/j.rse.2011.06.005.

Rautiainen, M., Lukeš, P., 2015. Spectral contribution of understory to forest reflectance in a boreal site: an analysis of EO-1 Hyperion data. Remote Sens. Environ. 171, 98–104. https://doi.org/10.1016/j.rse.2015.10.009.

Rouse Jr., J.W., Haas, R.H., Schell, J.A., Deering, D.W., 1974. Monitoring vegetation systems in the Great Plains with ERTS. NASA, Goddard Space Flight Center Third ERTS-1 Symposium 1 (A), 309–317.

Schaepman-Strub, G., Schaepman, M.E., Painter, T.H., Dangel, S., Martonchik, J.V., 2006. Reflectance quantities in optical remote sensing – definitions and case studies. Remote Sens. Environ. 103 (1), 27–42. https://doi.org/10.1016/j.rse.2006.03.002.

Tonteri, T., Salemaa, M., Rautio, P., Hallikainen, V., Korpela, L., Merilä, P., 2016. Forest management regulates temporal change in the cover of boreal plant species. Forest Ecol. Manag. 381, 115–124. https://doi.org/10.1016/j.foreco.2016.09.015.

Ustin, S.L., Ruaño, D., Hunt, E.R., 2012. Estimating canopy water content from spectroscopy. Israel J. Plant Sci. 60, 9–23.

Yang, W., Kobayashi, H., Suzuki, R., Nasahara, K.N., 2014. A simple method for retrieving understory NDVI in sparse needleleaf forests in Alaska using MODIS BRDF data. Remote Sens. 6 (12), 11936–11955. https://doi.org/10.3390/rs61211936.

Ziph-Schatzberg, L., Wiggins, R., Woodman, P., Saleh, M., Nakanishi, K., Soletsky, P., Goldstein, N., Fox, M., Tannian, B., 2018. Compact visible to extended-SWIR hyperspectral sensor for unmanned aircraft systems (UAS). In: Proc. SPIE 10644, Algorithms and Technologies for Multispectral, Hyperspectral, and Ultraspectral Imagery XXIV. 106441. https://doi.org/10.1117/12.2305615.